

# Coupling Reduction and the Higgs Mass

N.D.Tracas<sup>(1)</sup>, G. Tsamis<sup>(1)</sup>, N.D. Vlachos<sup>(2)</sup> and G. Zoupanos<sup>(1,3)</sup>

<sup>1</sup>Physics Department, National Technical University,  
GR-157 73 Athens, Greece

<sup>2</sup>Theoretical Physics Division, Aristotle University,  
GR-54124 Thessaloniki, Greece

<sup>3</sup>Max-Planck-Institut für Physik,  
Föhringer Ring 6, 80805 München, Germany

and

Arnold-Sommerfeld-Center für Theoretische Physik,  
Department für Physik, Ludwig-Maximilians-Universität München,  
Theresienstrasse 37, 80333 München, Germany

## Abstract

Assuming the existence of a functional relation among the Standard Model (SM) couplings gauge  $\alpha_1$  and quartic  $\lambda$ , we determine the mass of the Higgs particle. Similar considerations for the top and bottom Yukawa couplings in the minimal supersymmetric SM lead to the prediction of a narrow window for  $\tan \beta$ , one of the main parameters that determine the light Higgs mass.

**1. Introduction.** Copious theoretical efforts to establish a deeper understanding of Nature, led to very interesting constructions such as Superstring Theories that aim to unify consistently all interactions. The main goal expected from a unified description of interactions by the Particle Physics community is to understand the present day large number of free parameters of the Standard Model (SM) in terms of a few fundamental ones. Realistically, one expects to achieve at least a partial *reduction of couplings*. Indeed, the celebrated SM had so far outstanding successes in all its confrontations with experimental results. However, its apparent success is spoiled by the presence of a plethora of free parameters mostly related to the ad-hoc introduction of the Higgs and Yukawa sectors in the theory.

Towards reducing the independent parameters of a theory, a method has been developed which looks for renormalization group invariant (RGI) relations [1–9, 11] holding below the Planck scale, which in their turn are preserved down to Grand Unified (GUT) or lower scales. This program applied to dimensionless couplings of supersymmetric GUTs, such as gauge and Yukawa couplings, had already noticeable successes by predicting correctly, among other things, the top quark mass in the finite and in the minimal  $N = 1$  supersymmetric SU(5) GUTs [1, 2]. An interesting prediction of the lightest Higgs mass in a  $N=1$  Finite SU(5) GUT [1] will be confronted with the experiment soon. An impressive aspect of the RGI relations is that one can guarantee their validity to all-orders in perturbation theory by studying the uniqueness of the resulting relations at one-loop, as was proven in the early days of the couplings reduction program [5]. Even more remarkable is the fact that it is possible to find RGI relations among couplings that guarantee finiteness to all-orders in perturbation theory [9](see also [10]). Here, we would like to examine to which extent the above method can be applied to minimal schemes such as the SM and its minimal supersymmetric extension, the MSSM. In fact, the former, was one of the first applications of the above reduction scheme [6, 8, 11] assuming a perturbative ansatz. The implications of a stronger condition have been examined in ref [12].

Let us first recall some basic issues concerning the reduction of couplings. A RGI relation  $\Phi(g_1, \dots, g_N) = 0$ , has to satisfy the partial differential equation  $\mu d\Phi/d\mu = \sum_{i=1}^N \beta_i \partial\Phi/\partial g_i = 0$ , where  $\beta_i$  is the  $\beta$ -function of  $g_i$ . There exist  $(N - 1)$  independent  $\Phi$ 's, and finding the complete set of these solutions is equivalent to solve the so-called reduction equations (REs),  $\beta_g(dg_i/dg) = \beta_1$ ,  $i = 1, \dots, N$ , where  $g$  and  $\beta_g$  are the primary coupling and its  $\beta$ -function correspondingly. Using all the  $(N - 1)\Phi$ 's to impose

RGI relations, one can, in principle, express all the couplings in terms of a single coupling  $g$ . The complete reduction, which formally preserves perturbative renormalizability, can be achieved by demanding a power series solution, where its uniqueness can be investigated at the one-loop level. The completely reduced theory contains only one independent coupling with the corresponding  $\beta$ -function. This possibility of coupling unification is attractive, but it can be too restrictive and hence unrealistic. To overcome this problem, one may use fewer  $\Phi$ 's as RGI constraints.

After investigating specific examples, it becomes clear that the various couplings in supersymmetric theories have easily the same asymptotic behavior. Therefore, searching for a power series solution to the REs is justified. This is not the case in non-supersymmetric theories. Still in the SM  $\alpha_3$  and  $\alpha_2$  have the same behavior but one cannot be reduced in favor of the other [11]. Here, we will examine in some detail the possibility to reduce the couplings  $\alpha_1$  and the scalar quartic coupling  $\lambda$  of the SM, which have the same asymptotic behavior too.

As already mentioned, the method of reduction was applied in the couplings of the SM in refs [6, 8, 11]. The predictions for the Higgs boson mass in ref [6, 8] and for the Higgs and the top quark masses in ref [11] did not survive confrontation with experiment. In the present work, after studying the evolution of the SM couplings under the renormalization group flow, we look for solutions of the reduction equations following ref [1–5, 8, 9, 11] by generalizing their perturbative ansatz. Eventually, we are led to the updated solutions of ref [6] and a Higgs mass prediction in a region that is currently under experimental investigation, which we do not consider as totally conclusive yet. If the experimental results persist as in [13] when better statistics are available, then we will consider the SM case as an educative example and a motivation for applying our method in MSSM, which is examined here too.

**2. *Studies of the behavior of the couplings under RGEs.*** In the following, we will investigate the behavior of the SM and MSSM couplings under the renormalization group equations in order to establish a possible realisation of the reduction scenario. The most promising case appears to connect the scalar quartic coupling  $\lambda$  and the U(1) gauge coupling  $\alpha_1$ . We expect that such a relation leads to a prediction of the Higgs mass. Let us start with the 1-loop contributions. At this level, the RGE's for the gauge and

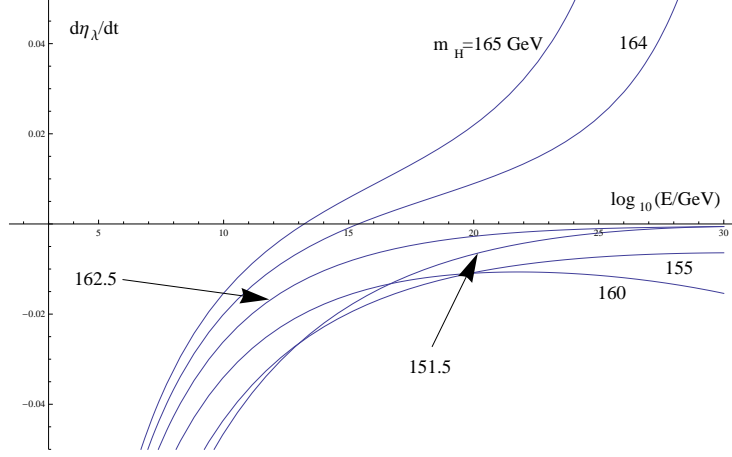


Figure 1: Plotting the derivative  $d\eta_\lambda/dt$  as a function of  $t$

the (top) Yukawa <sup>1</sup> can be solved analytically. The running of the quartic coupling is governed by the equation

$$\frac{d\tilde{\lambda}}{dt} = \beta_\lambda = \frac{1}{2\pi} \left[ L_2 \tilde{\lambda}^2 + (A_{1L}\alpha_1 + A_{2L}\alpha_2) \tilde{\lambda} + A_{11}\alpha_1^2 + A_{12}\alpha_1\alpha_2 + A_{22}\alpha_2^2 + H_L\alpha_t\tilde{\lambda} + H_2\alpha_t^2 \right], \quad (1)$$

where

$$\begin{aligned} \tilde{\lambda} &= \frac{\lambda}{4\pi}, & \alpha_t &= \frac{h_t^2}{4\pi}, & t &= \ln(E), \\ L_2 &= 6, & A_{1L} &= -\frac{3}{2}, & A_{2L} &= -\frac{9}{2}, \\ A_{11} &= \frac{3}{8}, & A_{12} &= \frac{3}{4}, & A_{22} &= \frac{9}{8}, & H_L &= 6, & H_2 &= -6, \end{aligned}$$

and  $\alpha_i$ ,  $i = 1, 2, 3$  are the gauge couplings.

To check that the ratio  $\lambda$  over  $\alpha_1$  indeed tends to a constant value at high scales, we plot the derivative of the ratio  $\eta_\lambda \equiv \tilde{\lambda}/\alpha_1$  as a function of  $t$ , for several initial values of the  $\tilde{\lambda}$  coupling, which we trade for the (running) Higgs mass. In Fig.(1) we show such a plot. Starting from  $m_H = 165$  GeV, we see that the derivative is positive for high energies. Upon lowering the Higgs

<sup>1</sup>Only the top Yukawa coupling is taken into account in the running.

mass, the derivative decreases and, for  $m_H \sim 162$  GeV, it goes asymptotically to zero. Further lowering the Higgs mass the derivative becomes negative but again for  $m_H \sim 151.5$  GeV goes once more asymptotically to zero. For even smaller values of the Higgs mass the derivative becomes positive but now  $\tilde{\lambda}$  passes through negative values<sup>2</sup>. Notice that the  $\eta_\lambda$  becomes constant at energies well above the Planck scale, however at the 2-loop order the situation improves appreciably. Let us explore the above situation a bit further. We can easily express the running of the ratio  $\eta_\lambda$  in the form

$$\frac{d\eta_\lambda}{dt} = \frac{1}{\alpha_1} \frac{d\tilde{\lambda}}{dt} - \frac{\tilde{\lambda}}{\alpha_1^2} \frac{d\alpha_1}{dt} = \frac{1}{\alpha_1} \beta_\lambda(\alpha_1, \alpha_2, \alpha_t, \tilde{\lambda}) - \frac{\tilde{\lambda}}{\alpha_1^2} \beta_1(\alpha_1), \quad (2)$$

where  $\beta_1$  is the 1-loop  $\beta$ -function for the  $\alpha_1$  coupling. This expression can be easily cast in the following form

$$\frac{d\eta_\lambda}{dt} = \alpha_1 \beta_\lambda(1, \alpha_2/\alpha_1, \alpha_t/\alpha_1, \eta_\lambda) - \alpha_1 \eta_\lambda b_1 \quad (3)$$

where  $\beta_1 = b_1 \alpha_1^2$ . Since at the 1-loop level the differential equations for the gauge and Yukawa couplings can be solved independently of the  $\tilde{\lambda}$  coupling, we can express  $\alpha_1$ ,  $\alpha_2$  and  $\alpha_t$  as functions of  $t$  and recast the above equation in the form

$$\frac{d\eta_\lambda}{dt} = \alpha_1(t) \beta_\lambda(t, \eta_\lambda) - \alpha_1(t) \eta_\lambda \beta_1(1) \equiv \alpha_1(t) F_{\eta_\lambda}(t, \eta_\lambda), \quad (4)$$

using the same symbol  $\beta_\lambda$  for the new function of  $t$  and  $\eta_\lambda$ . In Fig.2 we plot contours of constant value (-0.01, 0 and 0.01) for  $\alpha_1(t) F_{\eta_\lambda}(t, \eta_\lambda)$  in the  $(t, \eta_\lambda)$  plane. We clearly see that the zero value contour tends, for albeit very high energies, to a constant value for the ratio  $\eta_\lambda$  ( $\sim 1.3$  and  $\sim 0.05$ ).

Let us explore this situation from even another point of view and treat  $\alpha_1$ ,  $\alpha_2/\alpha_1 \equiv \eta_2$ ,  $\alpha_t/\alpha_1 \equiv \eta_t$  and  $\eta_\lambda$  as independent variables. Then we rewrite Eq.3 in the form

$$\frac{d\eta_\lambda}{dt} = \alpha_1 F_{\eta_\lambda}(\eta_2, \eta_t, \eta_\lambda) \quad (5)$$

using again the same symbol  $F_{\eta_\lambda}$ . The derivative of  $\eta_\lambda$  with respect to  $\alpha_1$  is given by

$$\frac{d\eta_\lambda}{d\alpha_1} = \frac{\frac{d\eta_\lambda}{dt}}{\frac{d\alpha_1}{dt}} = \frac{\alpha_1 F_{\eta_\lambda}(\eta_2, \eta_t, \eta_\lambda)}{b_1 \alpha_1^2} = \frac{F_{\eta_\lambda}(\eta_2, \eta_t, \eta_\lambda)}{b_1 \alpha_1}. \quad (6)$$

---

<sup>2</sup>Recall that the assumption the  $\lambda$  stays always positive, for the whole energy scale, gives a lower bound to the Higgs mass  $\sim 149$  GeV.

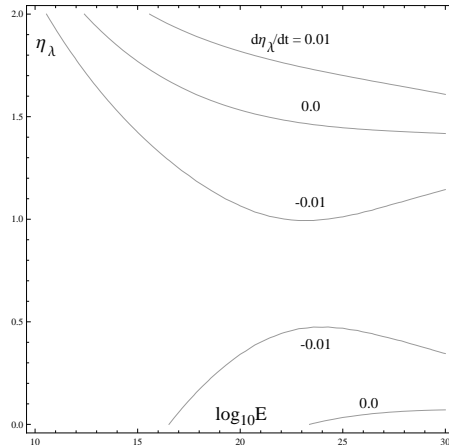


Figure 2: Contours of constant value of the derivative  $d\eta_\lambda/dt$  in the  $(t, \eta_\lambda)$  plane for three values: -0.01, 0 and 0.01

If  $\eta_\lambda$  tends to a constant value, then the above derivative should tend to zero. This is of course true when  $\alpha_1$  becomes very large but also when the numerator,  $F_{\eta_\lambda}(\eta_2, \eta_t, \eta_\lambda)$  is equal to zero. Just to have a first impression, we put  $\eta_2 = \eta_t = 0$  (both ratios tend to zero for very high energies). Then  $F_{\eta_\lambda}(0, 0, \eta_\lambda)$  is just a second order polynomial in  $\eta_\lambda$  with zeros at  $\sim 1.34$  and  $\sim 0.047$ , which are the two fixed points observed many years ago [6]. We can plot, in the space of  $(\eta_2, \eta_t, \eta_\lambda)$ , the surface where  $F_{\eta_\lambda}(\eta_2, \eta_t, \eta_\lambda) = 0$ . We can also numerically solve the differential equation and express  $\eta_\lambda$  as a function of  $t$ . Then we can make a parametric plot of the curve  $(\eta_2(t), \eta_t(t), \eta_\lambda(t))$ . We expect that for high energies, i.e. low values of  $\eta_2$  and  $\eta_t$ , the curve will lie on the surface  $F_{\eta_\lambda} = 0$ . This is shown in Fig.3. There are two surfaces corresponding to  $F_{\eta_\lambda} = 0$  and we have plotted the parametric curves for three Higgs masses. We clearly see that for the values  $m_H \sim 162.5$  and  $151.6$  GeV, the parametric curves lie on the surfaces for low values of  $\eta_2$  and  $\eta_t$ .

**3. The Reduction Equations.** The observations made in section 2 suggest that at least the couplings  $\tilde{\lambda}$  and  $\alpha_1$  are not independent in the SM and there may exist a functional relation among them at high scales. It is therefore justified to look for solutions of the reduction equation

$$\frac{d\tilde{\lambda}}{d\alpha_1} = \frac{\beta_\lambda}{\beta_1}. \quad (7)$$

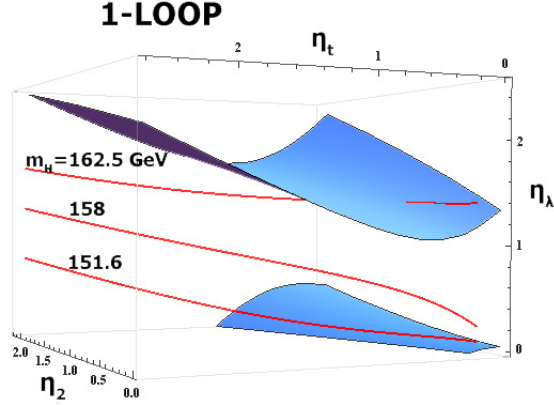


Figure 3: Surfaces of constant  $\eta_\lambda$  and parametric curves of  $(\eta_2(t), \eta_t(t), \eta_\lambda(t))$  for three values of the Higgs mass (1-loop).

Let us first look for solutions of Eq. 7 at 1-loop

$$\lambda(t) = c_1 \alpha_1(t), \quad (8)$$

where  $c_1$  would be a constant in the perturbative ansatz of ref [1–5, 8, 9, 11], but here we are searching for more general solutions. From the 1-loop  $\alpha_1(t)$  we can solve for  $t$  and express  $\alpha_2(t)$  and  $\alpha_t(t)$  (which are present in  $\beta_\lambda$ ) as functions of  $\alpha_1$ . Using the ansatz given in Eq.8, Eq.7 becomes a second order polynomial in  $c_1$ , where, of course, the coefficients depend on  $\alpha_1$ . In Fig.4 we plot the two solutions of the polynomial as a function of  $\alpha_1$ . We clearly see that for large values of  $\alpha_1$  (i.e. large energies), the two solutions tend to constant values. This is easily understood, since for high energies, we can neglect all the couplings but  $\alpha_1$  itself, and Eq.7 reduces to

$$c_1 = \frac{L_2 \alpha_1^2 c_1^2 + c_1 A_{1L} \alpha_1^2 + A_{11} \alpha_1^2}{b_1 \alpha_1^2} = \frac{L_2 c_1^2 + c_1 A_{1L} + A_{11}}{b_1} \quad (9)$$

with the two solutions being independent of  $\alpha_1$  (1.34233 and 0.0465609). We have already encountered this behavior when examining Eq.6. The second order polynomial above is the  $F_{\eta_\lambda}(0, 0, \eta_\lambda)$ . It is worth noting that the values of  $\alpha_1$ , when  $c_1$  approaches one of its fixed points correspond to energies well above the Planck scale. (At the Planck scale  $\alpha_1 \sim 0.017$ !).

We can go one step further and postulate that

$$\eta_\lambda = \frac{\tilde{\lambda}}{\alpha_1} = c_1 + c_2(\eta_2). \quad (10)$$

For high energies, the ratio  $\eta_2$  tends to zero and in order to obtain our first ansatz, we should require that  $c_2(\eta_2 \rightarrow 0) = 0$ . From Eqs.10 and 3 we easily get

$$\frac{dc_2}{dt} = \frac{d\eta_\lambda}{dt} = \alpha_1 \beta_\lambda(1, \eta_2, \eta_t, \eta_\lambda) - \alpha_1 \eta_\lambda b_1. \quad (11)$$

Writing

$$\frac{d\eta_2}{dt} = \frac{1}{\alpha_1} \frac{d\alpha_2}{dt} - \frac{\alpha_2}{\alpha_1^2} \frac{d\alpha_1}{dt} = \alpha_1 (b_2 \eta_2^2 - \eta_2 b_1), \quad (12)$$

where  $b_2$  is the one loop  $\beta$ -function coefficient for  $\alpha_2$ , and dividing the last two equations we get the derivative of  $c_2$  with respect to  $\eta_2$ . All that remains to be done is to express the ratio  $\eta_t$  as a function of  $\eta_2$ . Having the 1-loop analytical expressions for  $\alpha_t$  and  $\alpha_1$  as functions of  $t$ , we can substitute  $t$  from the relation

$$\eta_2 = \frac{\alpha_2}{\alpha_1} = \frac{\frac{\alpha_{20}}{1 - \frac{b_2}{2\pi} \alpha_{20}(t - t_0)}}{\frac{\alpha_{10}}{1 - \frac{b_1}{2\pi} \alpha_{10}(t - t_0)}} \rightarrow \quad (13)$$

$$t = t_0 + \frac{\eta_{20} - \eta_2}{\frac{1}{2\pi} [\eta_0 b_1 \alpha_{10} - \eta_2 b_2 \alpha_{20}]},$$

where  $\eta_{20} = \alpha_{20}/\alpha_{10}$  and  $\alpha_{10}$  and  $\alpha_{20}$  are the corresponding values at the scale  $t_0$ . Substituting  $\eta_\lambda = c_1 + c_2(\eta_2)$  and solving the differential equation

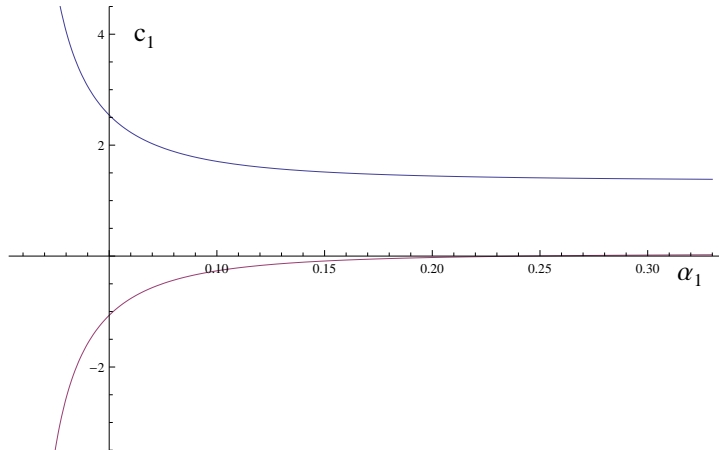


Figure 4: The “constant”  $c_1$  as a function of  $\alpha_1$



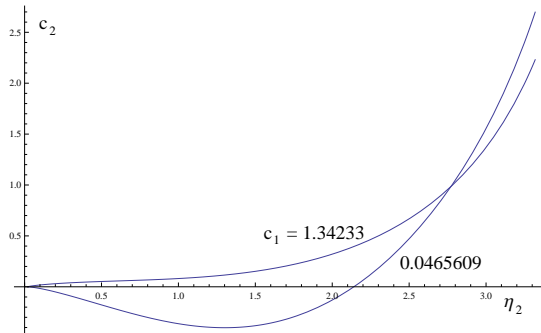


Figure 5: Plotting of  $c_2$  as a function of  $\eta_2$  for the two values of  $c_1$  (1-loop)

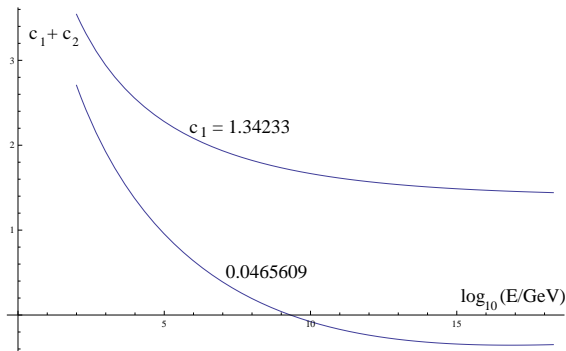


Figure 6: Plotting of  $c_1 + c_2 = \eta_\lambda$  as a function of  $\log_{10}(E)$  for the two values of  $c_1$  (1-loop)

for  $c_2(\eta_2)$ , we get  $c_2(\eta_2)$ . In Fig.5 we show the solutions for the two choices of  $c_1$  using the initial condition  $c_2(\eta_2 = 0.2) = 0$  (see Fig.4). In Fig.6 we show  $c_1 + c_2$  (i.e.  $\eta_\lambda$ ) as a function of the energy scale. The curve which corresponds to the higher  $c_1$  value has almost reached that value at the Planck scale, while the one that corresponds to the lower  $c_1$  value, apart from passing through unacceptable negative values, is still far away from that value. In Fig.7 we plot the function  $(c_1 + c_2(t))\alpha_1(t)$ , i.e.  $\tilde{\lambda}(t)$  itself, for the higher  $c_1$  value curve. The corresponding running (pole<sup>3</sup>) Higgs mass is  $\sim 162(154)$  GeV.

Going to 2-loop order, we should first determine the value(s) of the constant  $c_1$  in Eq.8. In this order, the procedure of keeping only the large terms

---

<sup>3</sup>For the known value of the top mass and the specific region of the Higgs mass, the Higgs pole mass is lower than the running mass by an amount of  $\sim 4.6 - 4.7\%$ . The relation between running and pole mass can be found in the references [14].

in the high-energy regime, does not lead to an independent from  $\alpha_1$  value(s)  $c_1$ . Nevertheless, for a big range of  $\alpha_1$ ,  $c_1$  varies by less than 5% from the 1-loop case: 0.0448 - 0.0465 for the lower value and 1.342 - 1.395 for the higher one. We solve now the 2-loop differential equation for  $c_2$  using as an initial value of  $\eta_\lambda$  at (very) high energies (i.e. low value of  $\eta_2$ ) the value  $c_1 = 1.395$ . The new value drives the ratio  $\eta_\lambda$  to its constant value early on the energy scale (see Fig.8). To be more specific, we see that  $\eta_\lambda(M_{Planck}) = 1.459$  and it remains pretty stable for higher energies. The Higgs running (pole) mass is  $\sim 163(155)$  GeV. At the 2-loop level, the problem with the lower  $c_1$  value persists:  $\eta_\lambda$  passes through negative values.

**4. The MSSM case.** If we assume that the top and bottom Yukawa couplings are related, the reduction equation is

$$\frac{d\alpha_t}{d\alpha_b} = \frac{\beta_t}{\beta_b} = \frac{\alpha_t \left( 6\alpha_t + \alpha_b - c_i^{(t)} \alpha_i \right)}{\alpha_b \left( 6\alpha_b + \alpha_t + \alpha_\tau - c_i^{(b)} \alpha_i \right)},$$

where  $c_i^{(t)} = (13/30, 3/2, 8/3)$  and  $c_i^{(b)} = (7/30, 3/2, 8/3)$ . Let us ignore, for simplicity, the contribution of  $\alpha_\tau$  and the small difference between  $c_1^{(t)}$  and  $c_1^{(b)}$ . Then, it is straightforward to deduce that if the ratio  $\alpha_t/\alpha_b$  is constant, then this ratio is equal to the corresponding ratio of the  $\beta$ -functions and is

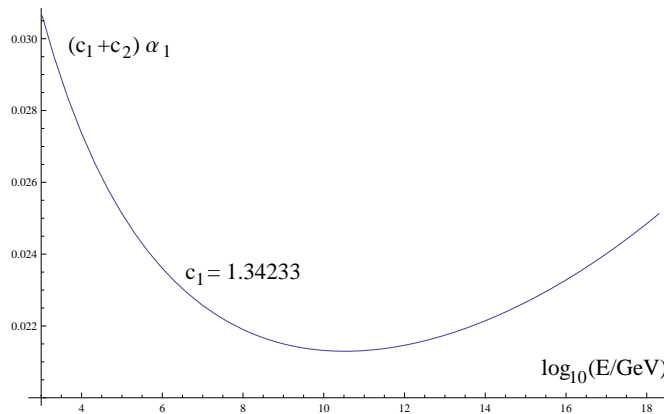


Figure 7: Plotting of  $(c_1 + c_2)\alpha_1 = \tilde{\lambda}$  as a function of  $\log_{10}(E)$  for the higher value of  $c_1$ . The corresponding running Higgs mass is  $\sim 162$  GeV (1-loop).

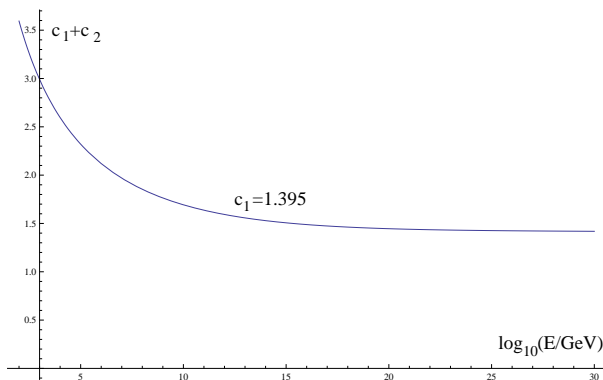


Figure 8: Plotting of  $\eta_\lambda$  as a function of  $\log_{10}(E)$  for  $c_1 = 1.395$ . The corresponding running (pole) Higgs mass is  $\sim 163(155)$  GeV (2-loop running).

equal to 1.

$$\frac{d}{dt} \left( \frac{\alpha_t}{\alpha_b} \right) = 0 \rightarrow \frac{1}{\alpha_b^2} (\alpha_b \beta_t - \alpha_t \beta_b) = 0 \rightarrow \frac{\alpha_t}{\alpha_b} = \frac{\beta_t}{\beta_b}.$$

This result combined with the previous equation leads to

$$6\alpha_t + \alpha_b - c_i^{(t)} \alpha_i = 6\alpha_b + \alpha_t + \alpha_\tau - c_i^{(b)} \alpha_i \rightarrow \alpha_t = \alpha_b.$$

That is, if we start with equal  $\alpha_t$  and  $\alpha_b$  at an energy scale, equality will remain for all energies. Putting back the  $\tau$  Yukawa coupling and the difference between the  $c_1^{(t)}$  and  $c_1^{(b)}$  constants, we expect a small deviation from that behavior.

Therefore, the procedure is the following: we start the running (with the SM RGEs) from the known values of the top-, bottom- and tau-mass. At  $M_{SUSY}$ , we choose the appropriate  $\tan\beta$  value that keeps the ratio  $\alpha_t/\alpha_b$  constant for all energies. Of course, we expect<sup>4</sup> this constant to be near 1.

In the MSSM scenario, at the scale  $M_{SUSY}$ , we have the relations

$$\begin{aligned} \alpha_t(SM) &= \alpha_t(MSSM) \sin^2 \beta \\ \alpha_b(SM) &= \alpha_b(MSSM) \cos^2 \beta \\ \alpha_\tau(SM) &= \alpha_\tau(MSSM) \cos^2 \beta. \end{aligned} \tag{14}$$

<sup>4</sup> The fact that  $\tan\beta$  could be predicted using reduction of couplings was suggested in [4] in a discussion with a different focus.

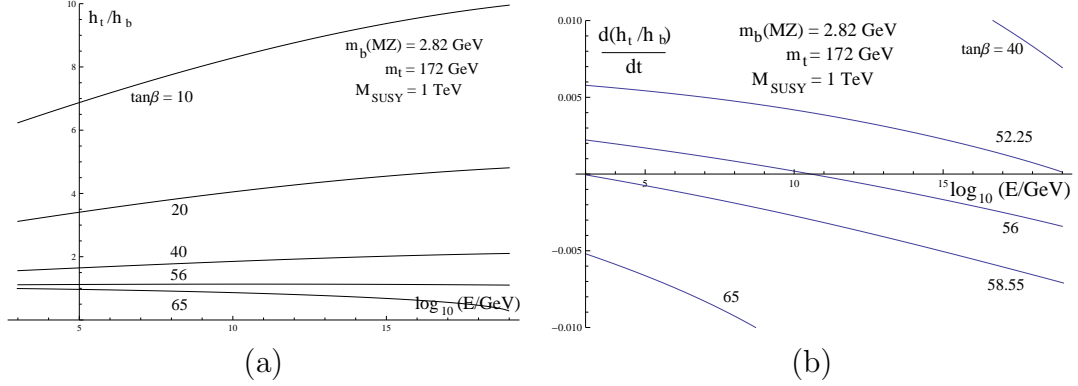


Figure 9: (a) The ratio  $h_t/h_b$  and (b) the derivative of the ratio as a function of energy for several values of  $\tan\beta$  and  $M_{SUSY} = 1$  TeV,  $m_t = 172$  GeV and  $m_b(M_Z) = 2.82$  GeV.

Above the  $M_{SUSY}$  scale, the running of all the parameters obeys the MSSM renormalization group equations, while below that scale, the SM regime is active.

In Fig.9 we plot the ratio  $h_t/h_b$  (a) and the derivative of the ratio (b) as a function of energy, for several values of  $\tan\beta$  and  $M_{SUSY} = 1$  TeV,  $m_t = 172$  GeV and  $m_b(M_Z) = 2.82$  GeV. We clearly see that for the range  $\tan\beta = 52.25 - 58.55$ , the derivative of the ratio stays almost zero (actually less than  $6 \cdot 10^{-3}$ ). The two values of  $\tan\beta$ : 52.25 and 58.55, are the limiting cases. For values below the first one, the derivative stays positive, while above the second one the derivative stays negative for the whole energy range.

In Fig.10 we plot the ratio  $h_t/h_b$  (in (a) and (c)) as well as the derivative of the ratio (in (b) and (d)) as a function of energy for the central value of  $\tan\beta = 56$ . In (a) and (b) we show three curves corresponding to  $M_{SUSY} = 1, 5$  and  $10$  TeV, keeping the masses of top and bottom at their central values. In (c) and (d) we vary the bottom mass  $m_b(M_Z) = 2.75, 2.82$  and  $2.89$  GeV, keeping the top mass at its central value and  $M_{SUSY} = 1$  TeV. The differences upon varying the top mass are negligible.

Now, using the program SUSPECT [15]<sup>5</sup>, we can plot in the plane of  $(m_0, m_{1/2})$  contours of constant (pole) mass values for the lightest supersym-

<sup>5</sup>We run the program using the mSUGRA model, 2-loop running and evaluation of pole masses. In all cases  $\text{sign}(\mu) = +1$ .

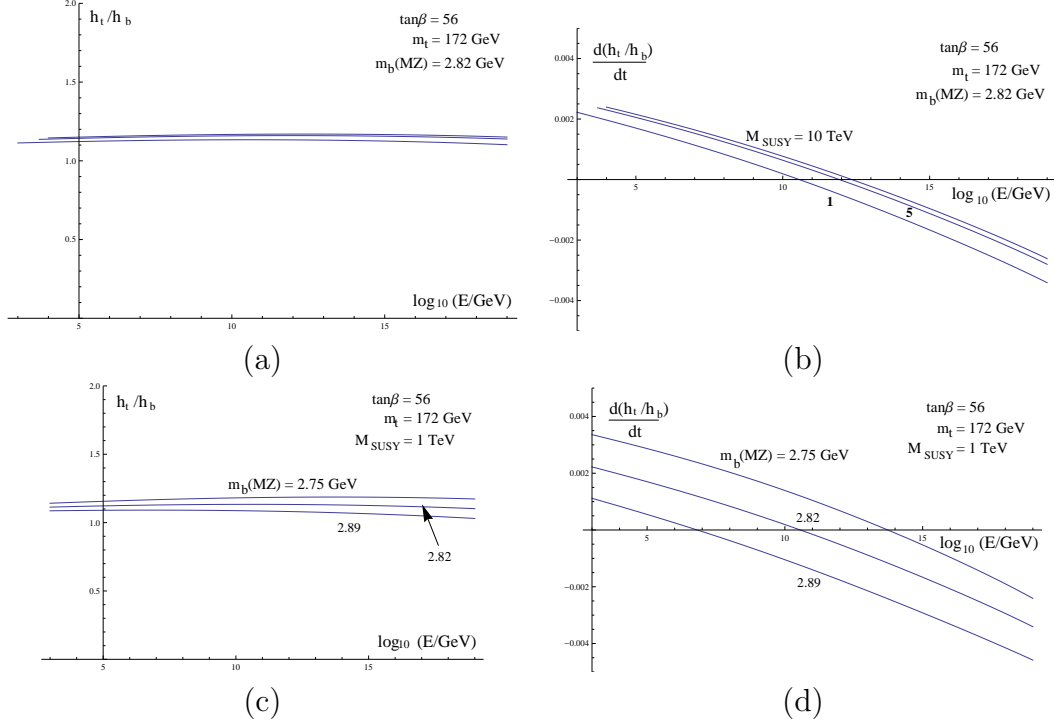


Figure 10: Plots of the ratio  $h_t/h_b$  ((a) and (c)) as well as the derivative of the ratio ((b) and (d)) as a function of energy for  $M_{SUSY} = 1, 5$  and  $10$  TeV ((a) and (b)) and varying the bottom mass in the experimental error region ((c) and (d)).

metric Higgs  $m_h$ <sup>6</sup> for  $\tan\beta = 56$ . In Fig.11 we show these contours for  $m_h = 114, 116, 118, 120$  GeV for initial  $A = 0$  GeV and  $\tan\beta = 56$ . The dotted-dashed contour corresponds to a gluino mass of 1 TeV, while the dashed contour to (the lightest) squark mass of 1.2 TeV. According to recent data from ATLAS/LHC and CMS/LHC [16], the two values represent the lower bounds for detection of the corresponding particle. Finally, in Fig.12 we plot the same contours for the two limiting  $\tan\beta$  cases: 58.55 and 52.25.

**5. Conclusions.** The idea of couplings reduction in a theory is very appealing since it increases its predictive power. Successful reduction led to all-loop finite theories and a prediction of the top-quark mass. The latter property was used as a selection criterion for a successful GUT. In the present

<sup>6</sup>We keep  $m_H$  for the SM Higgs and denote by  $m_h$  the lightest Higgs in the MSSM.

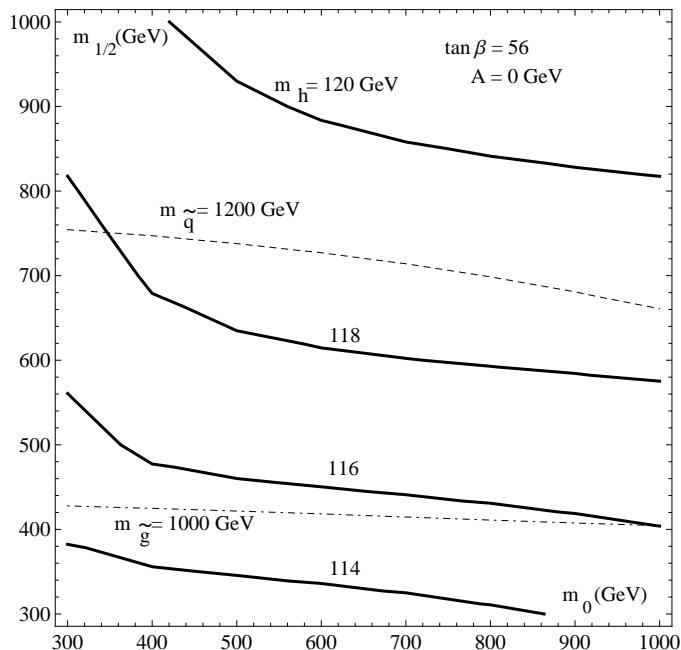


Figure 11: Contours of constant  $m_h$  (pole) mass in the plane of  $(m_0, m_{1/2})$  for initial value  $A = 0$  GeV and for  $\tan \beta = 56$ . The dashed and the dotted-dashed contours correspond to (lightest) squark and gluino masses of 1.2 TeV and 1 TeV correspondingly.

work, we have studied the reduction of certain couplings within the SM, and have obtained a prediction for the Higgs particle mass. Previous studies either overlooked this possibility, or did not include the heavy top-quark contribution. We have also started an analogous analysis in the MSSM, which we plan to extend in a forthcoming publication.

**Acknowledgements.** It is a pleasure to thank A. Djouadi, W. Hollik, S. Heinemeyer, L. Fayard, J. Kubo, E. Ma, M. Mondragon and W. Zimmermann for very interesting discussions. G.Z. is grateful to the Sommerfeld-LMU and MPI Munich the warm hospitality. This work was partially supported by the NTUA’s basic research support program “PEVE” 2009 and 2010 and the European Union ITN programme “UNILHC” PITN-GA-2009-237920.

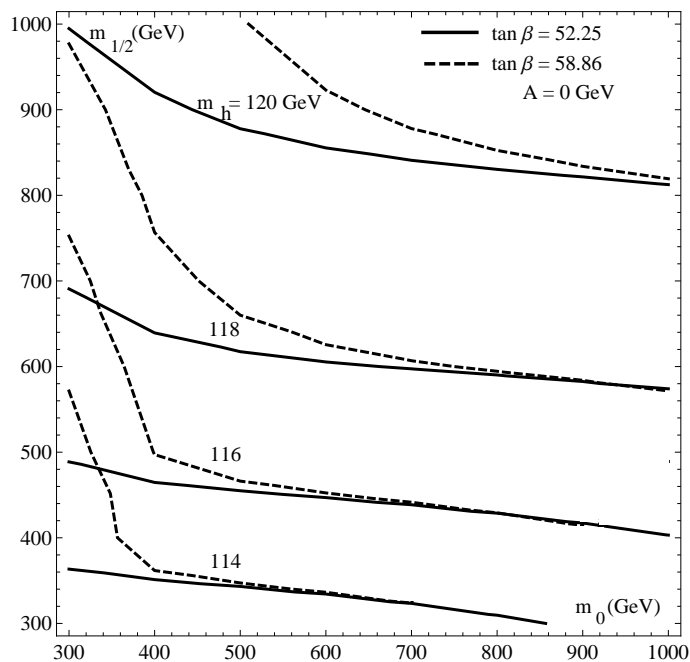


Figure 12: The same as in Fig.11 for the two limiting  $\tan \beta$  cases: 58.55 and 52.25

## References

- [1] D. Kapetanakis, M. Mondragon, and G. Zoupanos, Z. Phys. C60, 181 (1993), hep-ph/9210218;  
M. Mondragon and G. Zoupanos, Nucl. Phys. Proc. Suppl. 37C, 98 (1995);  
For an extended discussion and a complete list of references see: S. Heinemeyer, M. Mondragon and G. Zoupanos, SIGMA 6 (2010) 049, arXiv:1001.0428 [hep-ph].
- [2] J. Kubo, M. Mondragon, and G. Zoupanos, Nucl. Phys. B424, 291 (1994).
- [3] J. Kubo, M. Mondragon, N. D. Tracas, and G. Zoupanos, Phys. Lett. B342, 155 (1995), hep-th/9409003;  
J. Kubo, M. Mondragon, S. Shoda, and G. Zoupanos, Nucl. Phys. B469, 3 (1996), hep-ph/9512258;

- J. Kubo, M. Mondragon, and G. Zoupanos, Phys. Lett. B389, 523 (1996), hep-ph/9609218.
- [4] J. Kubo, M. Mondragon, M. Olechowski, and G. Zoupanos, Nucl. Phys. B479, 25 (1996), hep-ph/9512435.
- [5] W. Zimmermann, Commun. Math. Phys. 97, 211 (1985);  
R. Oehme and W. Zimmermann, Commun. Math. Phys. 97, 569 (1985).
- [6] E. Ma, Phys. Rev. D17, 623 (1978); E. Ma, Phys. Rev. D31, 1143 (1985).
- [7] N.P. Chang, Phys Rev D10 2706 (1974).
- [8] S. Nandi and W.-C. Ng, Phys.Rev. D20 (1979) 972.
- [9] C. Lucchesi, O. Piguet, and K. Sibold, Helv. Phys. Acta 61, 321 (1988);  
C. Lucchesi and G. Zoupanos, Fortschr. Phys. 45, 129 (1997), hep-ph/9604216.
- [10] A. V. Ermushev, D. I. Kazakov, and O. V. Tarasov, Nucl. Phys. B281, 72 (1987);  
D. I. Kazakov, Mod. Phys. Lett. A2, 663 (1987).
- [11] J. Kubo, K. Sibold, and W. Zimmermann, Nucl. Phys. B259, 331 (1985).
- [12] J. Iliopoulos, arXiv:hep-ph/0603146;  
B. Ananthanarayan, J. Pasupathy, Int. J. Mod. Phys. A17 335 (2002), hep-ph/0104286.
- [13] ATLAS NOTE, ATLAS-CONF-2011-135, September 30, 2011;  
CMS PAS HIG-11-022;  
Combined Standard Model Higgs boson searches with up to 2.3 fb<sup>-1</sup> of pp collision data at  $\sqrt{s} = 7$  TeV at the LHC, The ATLAS and CMS Collaborations, ATLAS-CONF-2011-157, CMS PAS HIG-11-023;  
G. Rolandi, Higgs Status (Tevatron+LHC) and combinations, Hadron-ColliderPhysics Symposium 2011, Paris, France;  
P. Jenni, The LHC Project and Discovery Physics, Proceedings of the Corfu Summer Institute, 2011 (to be published).
- [14] B. Schrempp and M. Wimmer, Prog. Part. Nucl. Phys. 37 1 (1996), hep-ph/9606386;



- A. Sirlin and R. Zucchini, Nucl. Phys. B266 389 (1986);  
J.A. Casas, J.R. Espinosa, M. Quiros and A. Riotto, Nucl. Phys. B436  
209 (1994); Erratum *ibid.* B439 466 (1995).
- [15] SuSpect: a program for the calculation of the SUpersymmetric particle  
SPECTrum, A. Djouadi, J.L. Kneur and G. Moultaka, hep-ph/0211331.
- [16] A. De Roeck, LHC: Searches for New Physics Beyond the Standard  
Model, Proceedings of the Corfu Summer Institute, 2011 (to be pub-  
lished).